Article

Not peer-reviewed version

InfraRed Thermographic Measurements in Parkinson's Disease Subjects

Antonio Cannuli *, Fabrizio Freni, Antonino Quattrocchi, Andrea Venuto, Roberto Montanini

Posted Date: 23 July 2024

doi: 10.20944/preprints202407.1861.v1

Keywords: infrared thermography; Parkinson's disease; autonomic dysfunction; thermoregulation

 doi:10.20944/preprints202407.1861.v1

Article

InfraRed Thermographic Measurements in Parkinson's Disease Subjects

Antonio Cannuli *, Fabrizio Freni, Antonino Quattrocchi, Andrea Venuto and Roberto Montanini

Department of Engineering, University of Messina, C.da di Dio, 98166 Messina, Italy
* Correspondence: acannuli@unime.it

Abstract: In this study, infrared thermography measurements were carried out to explore the physiological conditions of individuals diagnosed with Parkinson's disease. It is a complex neurodegenerative disorder that predominantly affects motor functions, significantly reducing the quality of life of affected people. However, in most cases, such disease is accompanied or preceded by non-motor manifestations, including autonomic dysfunction. Also known as neurovegetative dysautonomia, an autonomic dysfunction consists in a malfunction of the autonomic nervous system, which is also responsible for thermoregulation. In general, an autonomic dysfunction is not always easy to detect; a valid method could be represented by the vasomotor response of the skin to cold stimuli. In this context, infrared thermography can provide insights into the thermoregulatory patterns associated with autonomic dysfunction, representing a valuable tool for non-invasive assessment of Parkinson's research. Early biomarkers of the disease can be obtained through changes in skin temperature, allowing for timely intervention and management. The study was conducted on a cohort of 16 subjects, who were monitored with infrared images captured from their hands, following a specific protocol established by a preliminary analysis. Experimental results revealed that thermography can detect focal points and regions exhibiting either hyper- or hypo-thermia across the skin surface and muscular regions. This capability allows for extracting and categorizing precise medical data, difficult to determine during the early stages of the disease, thus facilitating ongoing monitoring efforts and early diagnosis in Parkinson research.

Keywords: infrared thermography; Parkinson's disease; autonomic dysfunction; thermoregulation

1. Introduction

The principle of InfraRed Thermography (IRT) is based on the physical phenomenon that any object with a temperature above absolute zero emits electromagnetic radiation. There exists a well-defined correlation between the surface temperature of an object and the intensity and spectral composition of the radiation it emits. IRT is a non-invasive technique that allows to detect such infrared radiation, emitted by the body and to convert it into the body temperature itself with distribution images called thermograms.

It is increasingly employed in a wide range of research fields, ranging from the constructions to the study of materials, from cultural heritage preservation to botany, from mechanical engineering to biomedicine and much more.

In biomedical field, for example, this technique is employed to detect skin temperature differences in real-time conditions and to identify possible signs of health disorder in the human body. Therefore, it can provide physiological information about the underlying structures, specifically in the diagnosis and the study of some diseases.

The first medical application dates back to 1956, when breast cancer patients were examined, for the first time, and asymmetric hot spots and vascularization points were found in infrared images of the breast [1]. Since then, its adoption has gradually increased, owing to the advancement of

 doi:10.20944/preprints202407.1861.v1

technology, which has become more affordable and user-friendly over the years. In addition, resolution, image size and portability have continually improved and, as a result, IRT imaging is now considered, a valuable and non-invasive tool in clinical practice [2–4]. Furthermore, by following a specific protocol, the results can objectively support the diagnosis of certain diseases and monitor physiological responses to various stimuli, such as thermal, chemical, or mechanical stress [2].

IRT is also successfully employed in vascular disorders, rheumatic diseases, tissue viability, oncology, dermatological and neonatal diseases, ophthalmology, surgery, fever screening and neurological disorders, including Parkinson's [5].

Parkinson's Disease (PD) is a progressive neurological disorder that affects the central and peripheral nervous system giving rise to bradykinesia, tremor, rigidity, and difficulty with balance and coordination. It is caused by a degeneration of dopaminergic neurons in substantia nigra, striatal projections and brain stem regions [6,7]. This neuronal loss leads to the reduction of nerve fibres essential for motor functions [8]. Pathogenesis associated with small nerve fibers in peripheral neuropathy reveals that the accumulation of pathological α-synucleine (phosphorylated) is a primary factor in neuronal death, which may explain the peripheral denervation observed in PD [9,10].

The symptoms usually start slowly and sometimes can drastically worsen over time. Early diagnosis plays a critical role in effective disease management and its delayed progression. The principal diagnosis is clinical, mainly based on motor symptoms. However, in a large part of cases, it is accompanied or preceded by non-motor manifestations, including autonomic dysfunctions [11] such as constipation, sialorrhea or reduced salivary secretion, urinary dysfunction, i.e. urge/incontinence, orthostatic hypotension, excessive sweating and dysfunctions in the thermoregulation. Both motor and non-motor manifestations are generally an expression of the intraneuronal protein accumulation, pathognomonic of the pathology in question. In fact, this phenomenon manifests itself at both the central and peripheral nervous system level and these non-motor symptoms can precede the onset of motor symptoms by many years as well as constitute a source of disability and reduced quality of life [4,5].

Autonomic dysfunction in PD patients can result in vasoconstriction [12]. In the early stages of PD, this dysfunction disrupts the regulation of body temperature due to excessive vasoconstriction. Autonomic dysfunction is a critical non-motor phenotype of PD. Recent literature suggests that it may serve as a potential biomarker for the early diagnosis of PD [13].

However, an autonomic dysfunction is not always easy to detect; a method could be represented by skin vasomotor response to cold stimuli.

IRT permits to investigate the involvement of the peripheral autonomic nervous system in PD, which may manifest as an altered cutaneous thermoregulation of the patient's skin after a thermal stress.

It is possible to evaluate alterations in skin thermoregulation and identify variations in trigger points and areas of hyper- and hypothermia. This approach could facilitate the extrapolation and classification of specific medical data regarding patients' health status, thereby enhancing the understanding and management of Parkinson's disease.

The scientific literature is rather sparse regarding studies that examine skin abnormalities in relation to peripheral autonomic dysfunction. One study investigated variations in blood flow regulation at the peripheral limb level in patients with PD [13]. Other research has highlighted discrepancies in skin temperature recovery in Parkinsonian patients using thermography [14,15]. Additionally, a further study analyzed distinct cutaneous vasomotor responses to differentiate between early-stage Parkinson's disease and essential tremor [16]. However, none of the studies conducted to date have assessed whether alterations in peripheral nerve endings are present in naïve patients. If such alterations were identified, quantifying them could potentially allow their use as prodromal markers.

In this study, a cohort of 16 subjects underwent monitoring, with infrared images captured of their hands, following a specific protocol established by a preliminary analysis. Experimental results revealed that thermography can detect focal points and regions exhibiting either hyper- or hypo-thermia across the skin surface and muscular regions. This capability allows for extracting and

 doi:10.20944/preprints202407.1861.v1

categorizing precise medical data, difficult to determine during the early stages of the disease, thus facilitating ongoing monitoring efforts and early diagnosis in Parkinson research. Moreover, it is possible to extract prodromal biomarkers of the disease allowing timely intervention and management.

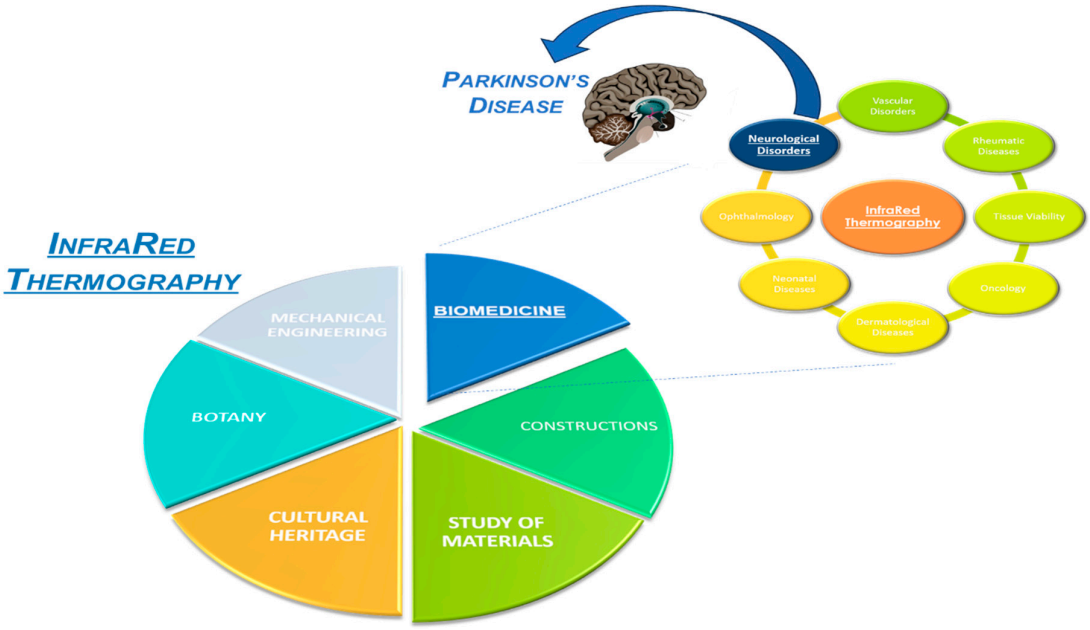

Figure 1. Applications of InfraRed Thermography.

2. Materials and Methods

2.1. Measurement Protocol

The measurement protocol hypothesized that the involvement of the peripheral autonomic nervous system in PD patients could be reflected in altered cutaneous thermoregulation. Therefore, it was proposed to assess cutaneous autonomic dysfunction using IRT before and after a thermal stress, i.e. Cold Stress Test (CST).

The protocol consisted of the following steps:

- The subject was instructed to sit in a thermo-regulated room of 10 m^2, after an acclimation of 15 minutes to an average temperature of 23 °C and a relative humidity of 60 %. The ambient temperature was recorded with a digital thermometer at the same time as the infrared measurements.
- The participant was asked to place his arms and hands, spaced 0.5 cm apart, focusing in a frontal view at the front of the camera, on a panel inclined at an angle of 20°, leaving the elbows to rest.
- It was recommended to remove any accessories such as rings or bracelets that could affect the measurement, causing unwanted reflections, with the aim of minimizing the impact of external sources that could lead to errors.
- After a waiting period of about 30 s, to stabilize the temperature of the hands, a first 20 s video was recorded and the temperature was averaged in order to determine the baseline temperature.
- Then, CST, i.e. the subject was instructed to immerse both hands, up to the wrist, wrapped in latex gloves, in a bowl of cold water at 10°C. Latex gloves were necessary to avoid subsequent evaporative cooling. Subject was previously recommended to report if it begins to feel pain due to cold water.
- After 2 min of immersion, the gloves were carefully removed from the hands without touching the skin.
- Immediately post-immersion, the skin temperature was continuously monitored from 0 to 10 min.

 doi:10.20944/preprints202407.1861.v1

After the measurement, a thermal imprint remains on the surface for a few minutes, it is therefore necessary to wait about 20 min for its disappearance before proceeding with the next measurement.

Different Regions Of Interest (ROI)s were investigated, the distal phalanx of each finger of the hand, more in detail the index, the middle, the ring and the little finger.

The study was conducted in accordance with the rules of Good Clinical Practice and current Legislation and in accordance with the current version of the Declaration of Helsinki. Medical guidelines have been followed [17].

2.2. Participants

The measurements were conducted on 16 different subjects, 8 Control Subjects (CSs), considered as reference of good health status and 8 subjects with PD diagnosis between 50 and 70 years of age. CSs were chosen based on the age and sex characteristics of the patients.

The exclusion criteria included subjects with diabetes mellitus, using vasoactive medicinal products, with presence of infection or fever before two weeks of testing, a previous history of recent acute myocardial infarction. Furthermore, subjects with no diagnosis of PD with concomitant diagnosis of neuropathies, any other neurological disorders, connective tissue diseases, endocrinopathies, such as thyroidopathies or diseases of the adrenal glands, arterial diseases, drug abuse that could affect skin temperature and then alter the measurement, were excluded.

Each participant was uniquely distinguished for the duration of the study by a three-digit code assigned sequentially from 001. The investigator recorded this code in the Case Report Form along with the subject name and associated identification number.

2.3. Experimental Setup

The experimental setup, shown in Figure 2, consisted of an infrared camera, model T650sc from FLIR Systems, a neoprene contrast panel and a computer for data processing and storage. A thermal camera is a device designed to detect electromagnetic radiation, which is naturally emitted by the human body, in the infrared spectrum. The T650sc is a high-performance thermal imaging camera meticulously engineered for research and scientific applications. It is equipped with an uncooled Vanadium Oxide (VOx) microbolometer detector that produces thermal images of 640 x 480 pixels, providing detailed thermal imagery within a spectral range of 7.5 to 14 μm. With a thermal sensitivity of less than 20 mK at 30 °C and a skin emissivity calibration of 0.987, it delivers precise temperature measurements. Its extensive temperature range of -40 to 150 °C enhances its versatility for a broad spectrum of uses, including industrial research, medical diagnostics, and scientific studies. Initially set to an acquisition frequency of 30 Hz for detailed observation of the phenomenon, the frequency was later reduced to 2 Hz to facilitate more manageable data processing.

The camera, inclined of 20°, was mounted on a tripod stand, adjusted to approximately 130 cm above the floor and 50 cm away from the sample. The neoprene panel was employed as a support for the hands, and its opacity was exploited to prevent unwanted reflections. The first problem in a thermographic measurement is to find a uniform surface, where to place the investigating sample, that can reduce undesirable reflections. For this purpose, after various tests with different materials, such as paper or wood, the neoprene panel was taken into consideration. It was tilted 20° to promote blood circulation for temperature recovery after CST.

Finally, the acquired IR images were processed using the ResearchIR software. The skin emissivity value was set to 0.987.

 doi:10.20944/preprints202407.1861.v1

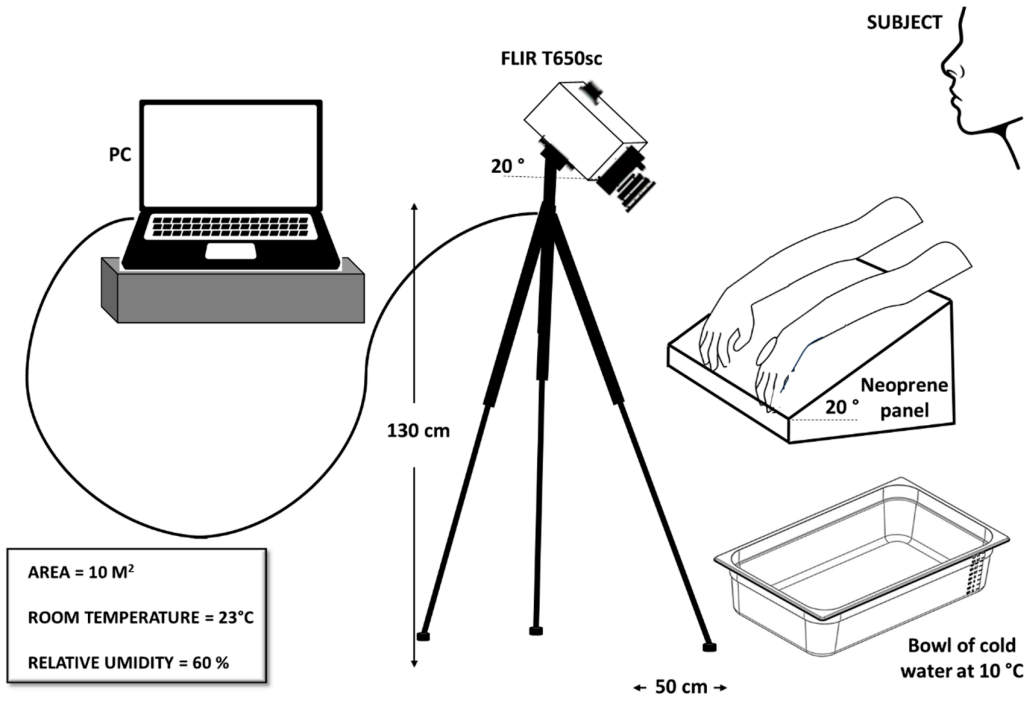

Figure 2. Sketch of the experimental setup.

3. Results

For brevity, only the results related to the right hands will be reported and finally a study of uncertainly between right and left hands will be presented.

3.1. Analyzed Parameters

1. In order to establish a preliminary parameter as prognostic marker of PD, the Thermal Recovery Ratio (TRR) for each ROI after 10 min was computed as a diagnostic measurement for vasoconstriction in the subjects. The calculation of TRR is depicted in the Equation 1 below as ratio of the difference between the temperature 10 min after CST and the temperature immediately afterwards the test ($T_{0\ post\ CST}$) and between the average of the baseline temperature acquired before CST and $T_{0\ post\ CST}$.
2. In order to minimize the error due to the thermal camera measurement in the temperature calculation, only the temperature differences were considered. Furthermore, after calculating the trend of the distribution of the temperature differences for the 4 individual ROIs, i.e. the TRR for the index, middle, ring and little fingers, the average of the 4 TRRs was calculated. Figure 3 shows the trend of the TRR as a function of the acquisition time for the individual ROIs considered. For brevity, the case relating to the right hand of a CS has been reported. The curves relating to the TRRs of the individual ROIs are shown in different colors, while the average of the 4 TRRs is represented in black with a dashed line.
3. This first parameter was then calculated, as represented in the equation below, thus trying to minimize the sources of error as much as possible.

$$TRR = \frac{T_{10_{post\ CST}} - T_{0_{post\ CST}}}{T_{\ baseline} - T_{0_{post\ CST}}}, \quad (1)$$

Preprints.org (www.preprints.org) | NOT PEER-REVIEWED | Posted: 23 July 2024 doi:10.20944/preprints202407.1861.v1

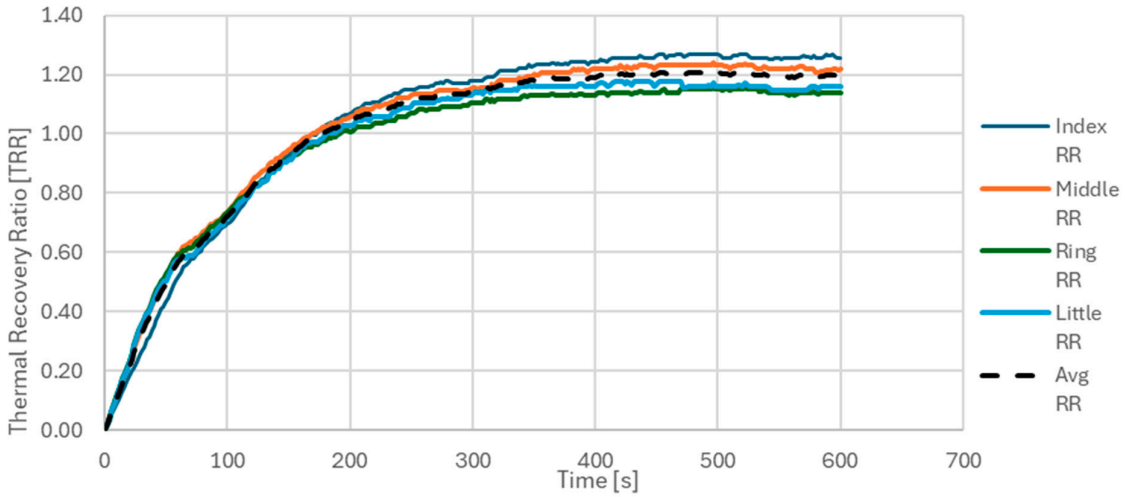

Figure 3. TRR as function of the acquisition time related to ROIs for a right hand of a CS; the black with dotted line represents the TRR average.

Another parameter calculated and taken into consideration as prognostic marker was INT, that is the area covered by the TRR average (f(t)), i.e. the integral divided by the number of considered points (N=600).

It is reported in Equation 2, as follows:

$$INT = \frac{1}{N}\int f(t)dt, \quad (2)$$

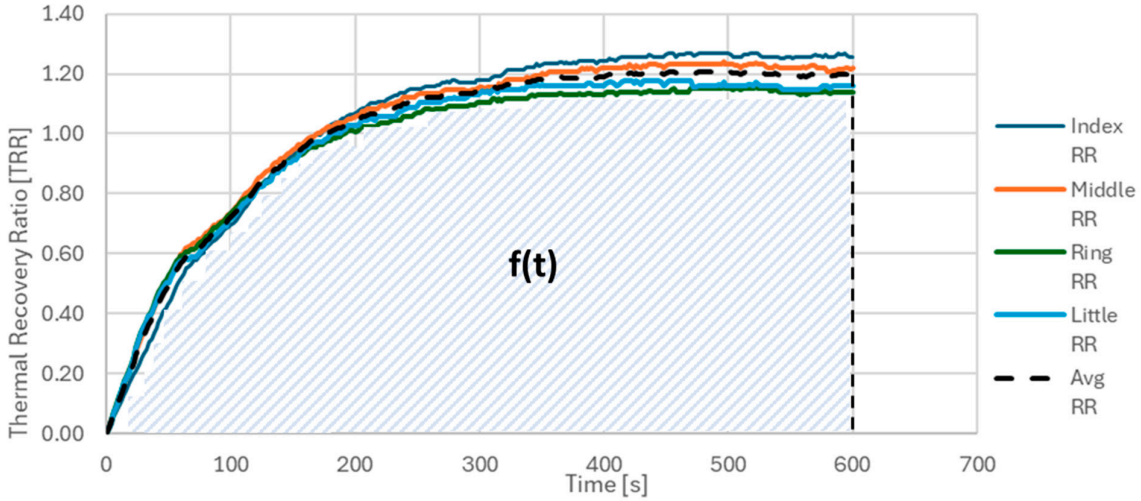

Figure 4. INT parameter calculated as the area covered by the TRR average, divided by the number of considered points.

3.2. Results

The Figure 5 shows respectively the thermographic images of a PD (on the top) and a CS subject (on the below) with a graduated scale of temperature between 18 and 36 °C. More in detail, the basal thermal distribution of the hands before the CST (Baseline, reported in the left), immediately afterwards the test ($T_{0\ post\ CST}$), after 5 min ($T_{5\ post\ CST}$) and 10 min of CST ($T_{10\ post\ CST}$).

 doi:10.20944/preprints202407.1861.v1

In the PD case, it is possible to appreciate by the thermographic view, how the hands show difficulties in thermoregulation, that is, an autonomic dysfunction in the thermal recovery, in fact they maintain a rather cold temperature.

As regards the case of CS, it is clear that there is no thermoregulatory problem, the subject has a normal trend of thermal recovery. The hands are completely heated after 10 min of CST.

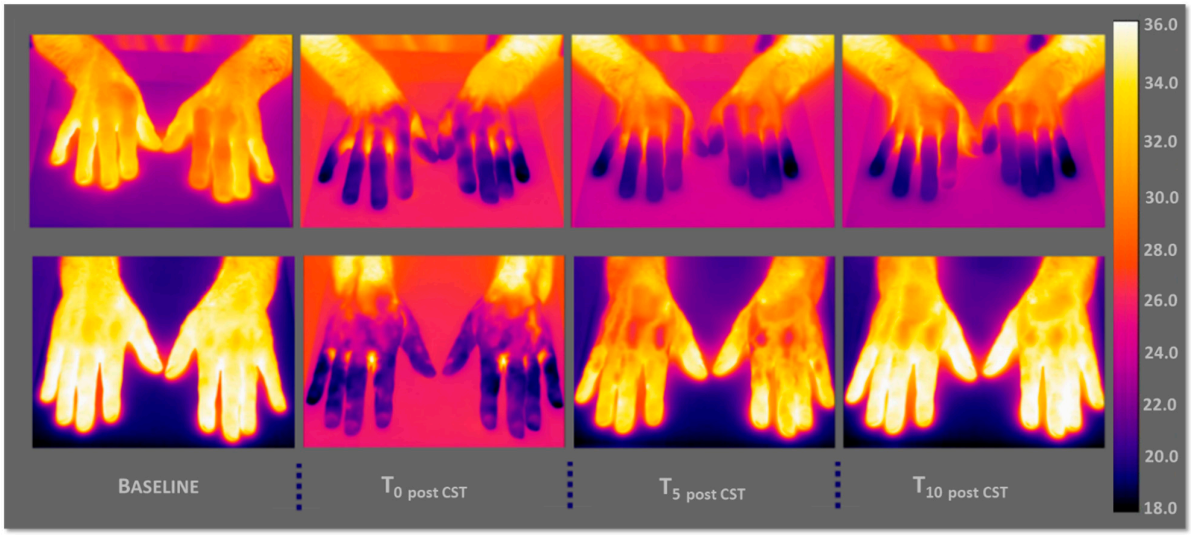

Figure 5. Thermal distribution of a PD (on the top) and a CS subject (on the below) with a graduated scale of temperature between 18 and 36 °C before the CST (Baseline, reported in the left), immediately afterwards the test ($T_{0\ post\ CST}$), after 5 min ($T_{5\ post\ CST}$) and 10 min of CST ($T_{10\ post\ CST}$).

Figure 6 reports the TRR average as function of the acquisition time calculated in the case of the right hand of a CS (orange line) and a PD (green line) with the corresponding thermal images at 0, post 5 min and 10 min after CST.

The PD case shows a different trend, that could be representative of an autonomic dysfunction. Specifically, the TRR maintains an almost constant temperature during the 10 min after CST. Furthermore, while in the CS case the max value is 1.2, in the PD case this value is 10 times less, i.e. 0.2.

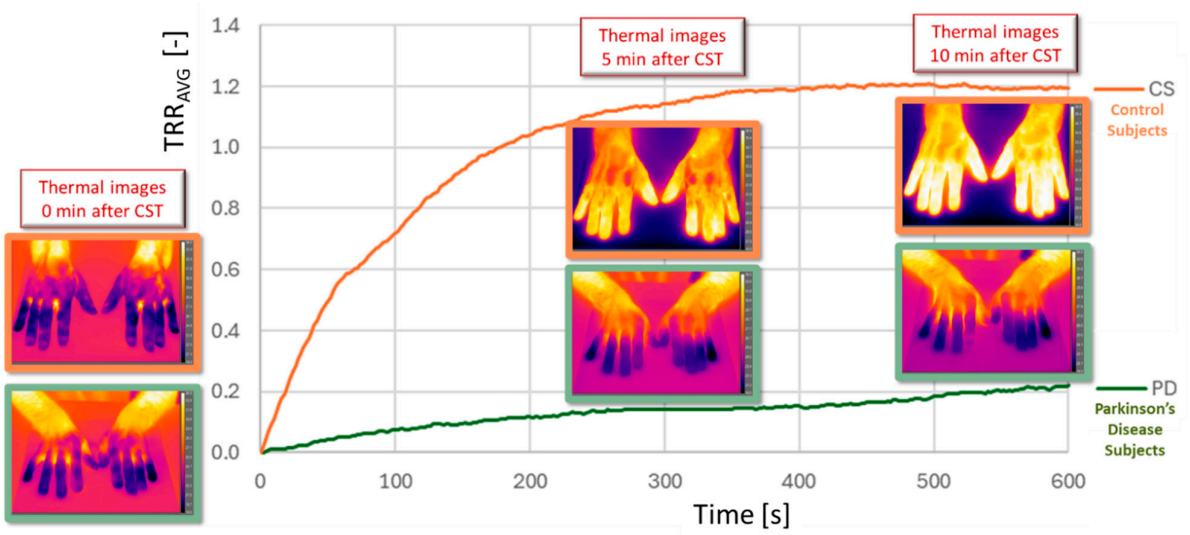

Figure 6. TRR average as function of the acquisition time with the corresponding thermal images at 0, post 5 min and 10 min after CST.

Preprints.org (www.preprints.org) | NOT PEER-REVIEWED | Posted: 23 July 2024 doi:10.20944/preprints202407.1861.v1

In Figures 7 and 8 are shown the TRR values as function of the acquisition time for all subjects, that is CS (Figure 7) and PD (Figure 8) subjects.

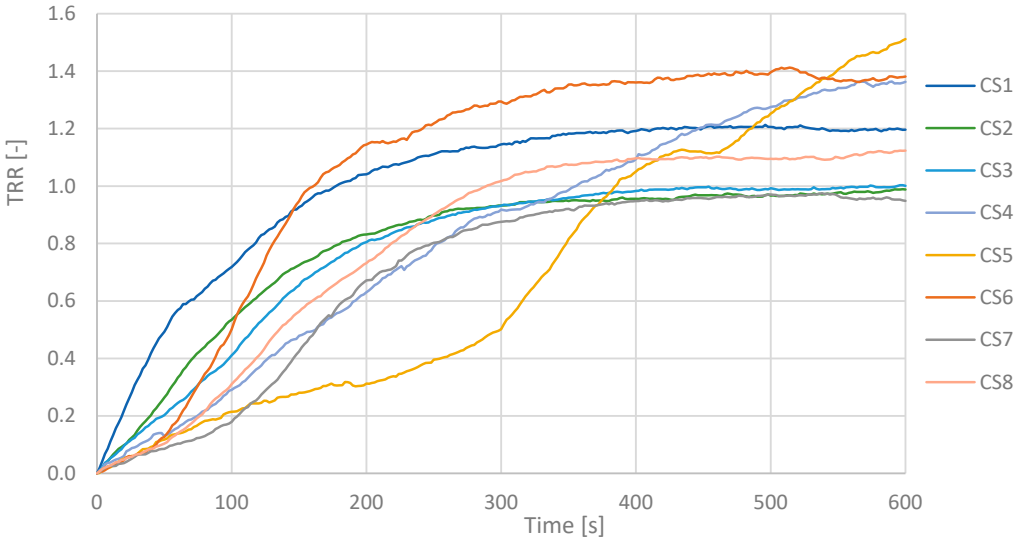

Figure 7. TRR as function of the acquisition time for CS subjects.

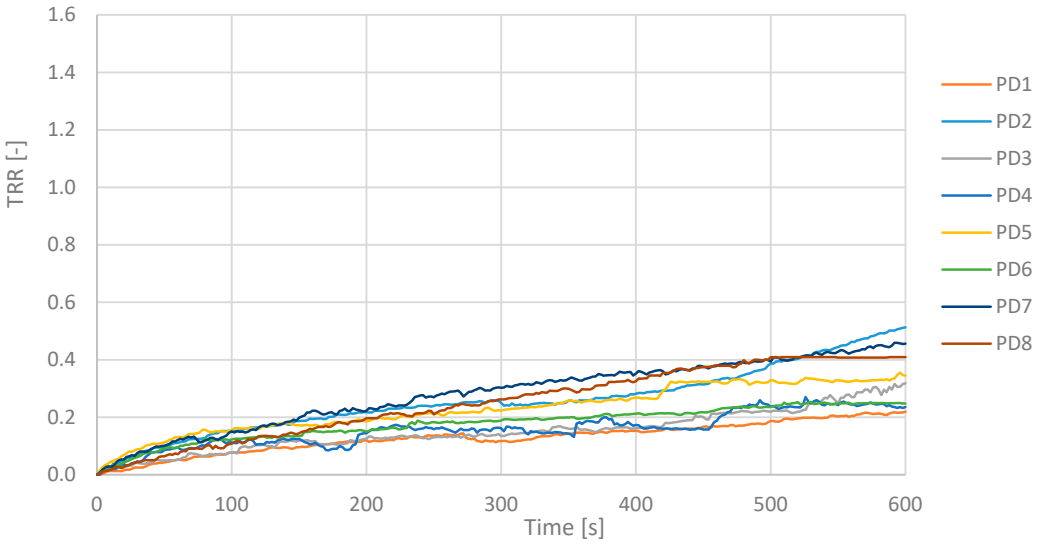

Figure 8. TRR as function of the acquisition time for PD subjects.

TRR is a parameter that in these measurements showed values less than 0.5 for an illness subject and greater than or next to 1.0 for a healthy subject. PD maintain fairly constant temperature values and show a low TRR. The mean value of the TRR has been calculated for all subjects, PD and CS subjects and reported in the histogram below.

Preprints.org (www.preprints.org) | NOT PEER-REVIEWED | Posted: 23 July 2024 doi:10.20944/preprints202407.1861.v1

Figure 9. Histogram representation of the TRR for PD and CS subjects.

The TRR for a PD subject shows values between 0.22 and 0.51 according to the severity of the disease, while in a CS next to or greater than 1.

Similar results also showed the second prognostic parameter, INT, shown in the scatter diagram of Figure 10.

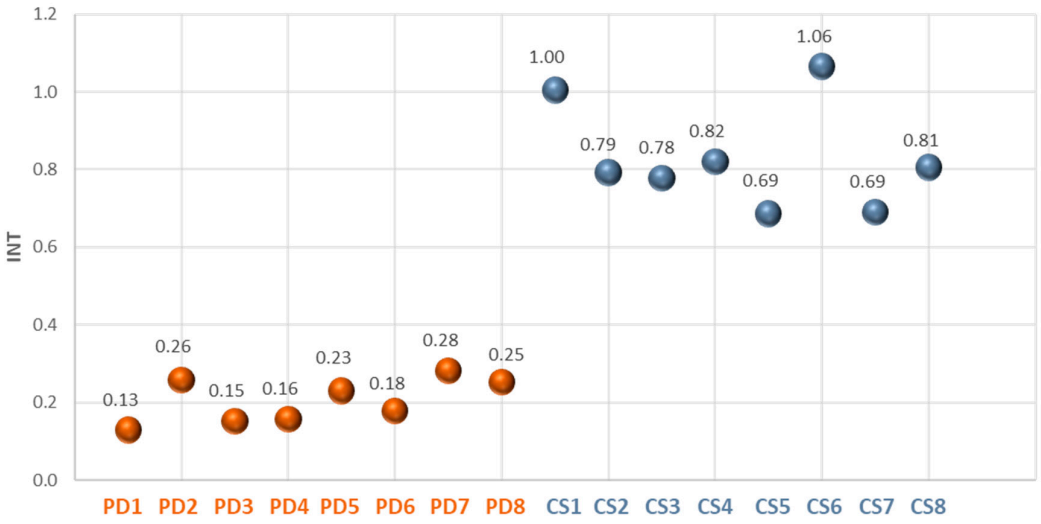

Figure 10. INT parameter for PD and CS subjects.

It is possible to establish a threshold value of 0.5 to differentiate between healthy and ill individuals. This parameter has also proven to be effective in distinguishing between the healthy and the ill.

3.3. Measurement Repeatability

Repeated measurements were also carried out on a healthy subject in order to study the uncertainty in the repeatability of the measurement.

Table 1 reports the value for the 4 measurements for the right and the left hand.

 doi:10.20944/preprints202407.1861.v1

Table 1. TRR calculated for 4 repeated measurements.

Thermal Recovery Ratio (TRR)		
	DX	**SX**
Measure 1	1.38	1.38
Measure 2	1.29	1.16
Measure 3	1.12	1.16
Measure 4	1.39	1.48
Mean (μ)	***1.30***	***1.29***
STD (σ)	***0.12***	***0.16***
Mean DX-SX ($\bar{x}$)	**1.30**	
STD DX-SX	**0.13**	

The results show as the TRR value is equal to ($\mu \pm \sigma$) = (1.30 ± 0.12) for the right hand (DX) and (1.29 ± 0.16) for the left hand (SX).

For the estimation of the uncertainty associated with the measurement, the UNI CEI ENV 13005 standard "Guide to the Expression of Uncertainty in Measurement" was followed. In this specific case, type A uncertainty was calculated, known as standard uncertainty, which is obtained through a posteriori statistical analysis of the results from repeated measurements. It is equal to the ratio of the standard deviation to the square root of the number of conducted tests (N=4) as follows:

$$u_A = \frac{\sigma}{\sqrt{N}} = \frac{0.13}{\sqrt{4}} = 0.065, \quad (3)$$

The total TRR value will be equal to $\bar{x} \pm u_A$ = 1.30 ± 0.065. After conducting repeated measurements and obtaining a mean value $\bar{x}$ and a standard uncertainty u_A, we can determine the extended uncertainty, U.

$$U = k * u_A = 3.18 * 0.065 = 0.21, \quad (4)$$

where the coverage factor, k, has been obtained from the *t-Student* probability density function, with 95% confidence level and 3 degrees of freedom.

Figures 11 and 12 report the TRR as function of the acquisition time for the 4 measurements related to the right and the left hand.

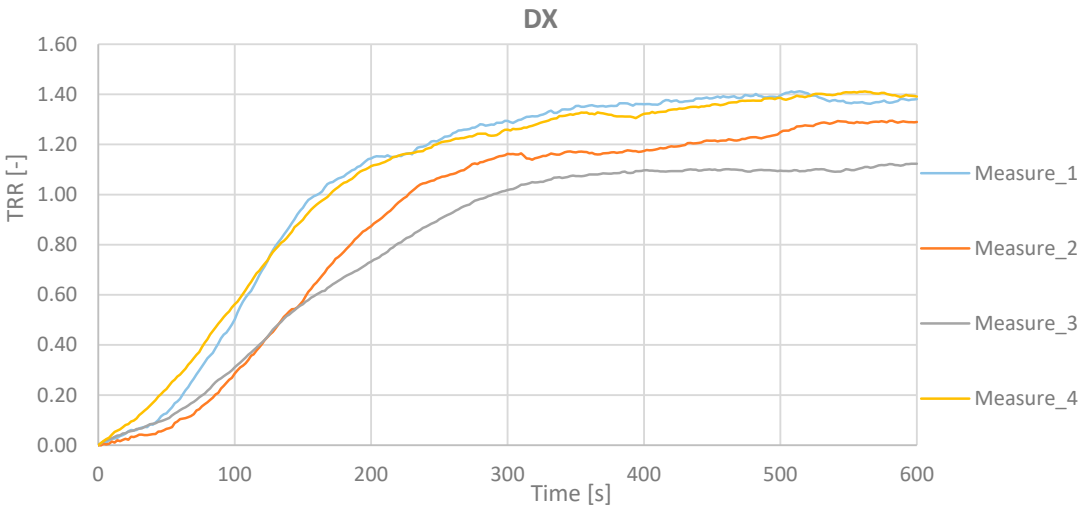

Figure 11. TRR as function of the acquisition time for the 4 measurements related to the right hand of the CS subject.

Preprints.org (www.preprints.org) | NOT PEER-REVIEWED | Posted: 23 July 2024 doi:10.20944/preprints202407.1861.v1

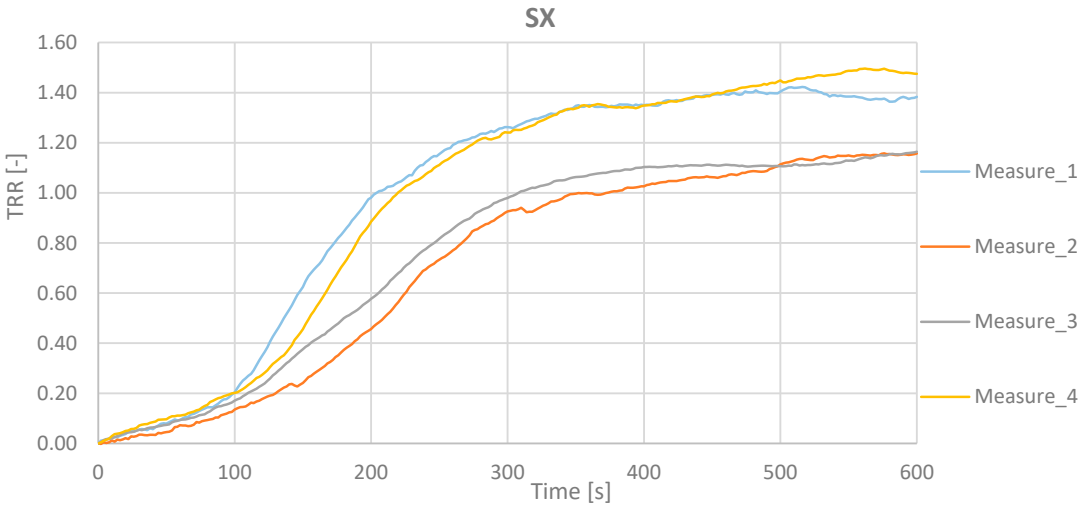

Figure 12. TRR as function of the acquisition time for the 4 measurements related to the left hand of the CS subject.

Figure 13 shows the TRR trend related to measurements made on the right hand and on the left hand for all subjects. These points shall fall within the uncertainty range of 0,21 represented by the two blue curves.

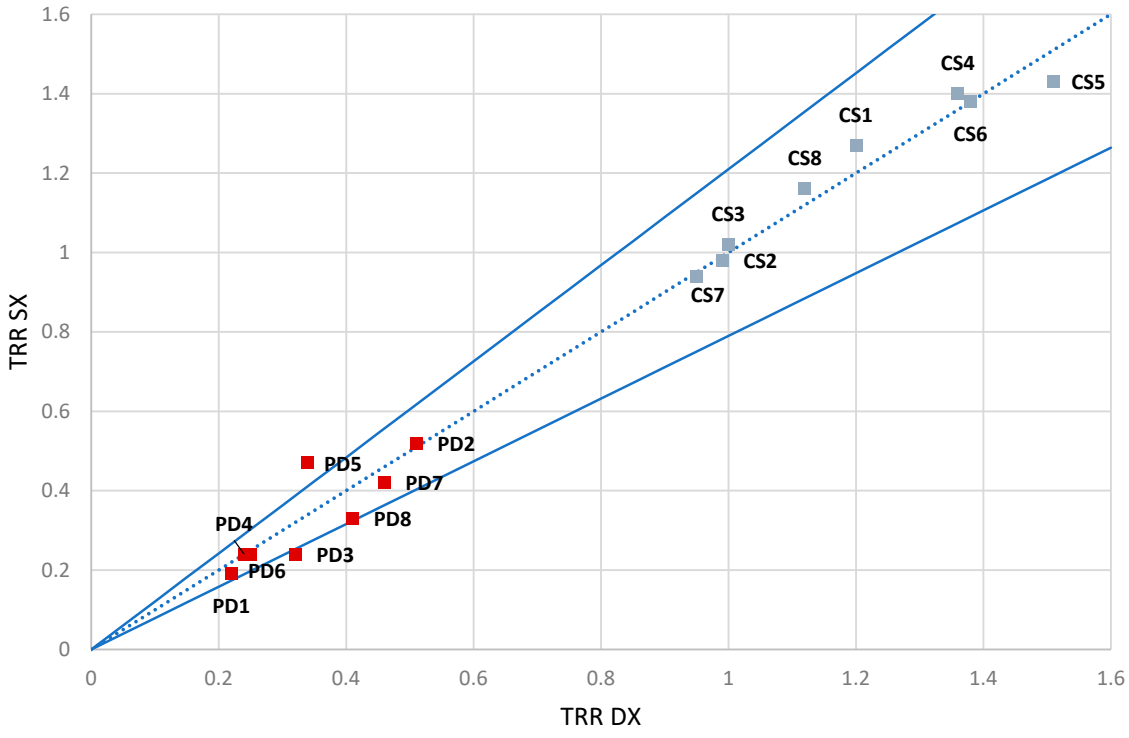

Figure 13. The TRR trend related to measurements made on the right hand and on the left hand for all subjects. These points shall fall within the uncertainty range of 0.21 represented by the two blue curves.

 doi:10.20944/preprints202407.1861.v1

4. Discussion

Compared to the measurements obtained from healthy subjects, it was expected that cutaneous thermographic analysis in Parkinson's patients would reveal altered autonomic innervation and an abnormal vasomotor reflex in the skin, as documented in PD literature [18]. Indeed, PD patients demonstrated abnormal cutaneous thermal responses, indicating cutaneous autonomic dysfunction.

Furthermore, it was expected that thermographic curves in PD analyses would exhibit a shallower slope, due to a reduced thermal recovery rate and so it was.

Additional parameters will be calculated to obtain a marker of the disease. Furthermore, it will be important to investigate the relationship between thermoregulation and motor asymmetry. The obtained data will then be correlated with scores from neuropsychological tests and clinical examinations. Ultimately, with a substantial number of measurements, it will be possible to develop a mathematical model that better approximates the calculated temperature distribution function, as has been done previously in other fields [19].

5. Conclusions

In conclusion, the presence of α-synuclein in PD patients induces vasoconstriction, leading to skin vasomotor dysfunction and reduced blood flow in the blood vessels, which results in cooling of the limbs. This vasoconstriction is due to autonomic dysfunction, a common occurrence in individuals with PD.

IRT shows significant promise as a valuable tool for assessing the health status of Parkinson's disease patients. Its ability to non-invasively detect and monitor autonomic dysfunction provides a complementary approach to traditional clinical evaluations.

Author Contributions: Conceptualization, R.M. and A.C.; methodology, R.M., A.C., F.F. and A.Q.; statistical analysis, A.C., F.F. and A.V.; investigation, A.C. and F.F.; data curation, A.C. and A.Q.; writing—original draft preparation, A.C.; writing—review and editing, R.M. and A.Q.; supervision, R.M. All authors have read and agreed to the published version of the manuscript.

Funding: This research received no external funding.

Data Availability Statement: Data will be made available upon reasonable request to the corresponding author.

Acknowledgments: We would like to thank all the subjects, PD and CS, included for their voluntary participation in this study.

Conflicts of Interest: The authors declare no conflicts of interest.

References

1. Lawson, R.. Implications of surface temperatures in the diagnosis of breast cancer. Can. Med. Assoc. J., **1956**, 75 (4), 309-310.
2. Strąkowska, M.; Strąkowski, R.; Strzelecki, M.; De Mey, G.; Więcek, B.. Thermal modelling and screening method for skin pathologies using active thermography. *Biocybern. Biomed. Eng.*, **2018**, 38 (3), 602-610.
3. Yousefi, B., Sharifipour, H.M., & Maldague, X.P.. A diagnostic biomarker for breast cancer screening via Hilbert embedded deep low-rank matrix approximation. *IEEE Trans. Instrum. Meas.*, **2021**, 70, 1-9.
4. Jones, B.F.. A reappraisal of the use of infrared thermal image analysis in medicine. *IEEE Trans. Med. Imaging*, **1998**, 17 (6), 1019-1027.
5. Borghammer, P.; Knudsen, K.; Brooks, D. J.. Imaging systemic dysfunction in Parkinson's disease. *Curr. Neurol. Neurosci. Rep.*, **2016**, 16 (6), 51.
6. Tanner, C.. Occupational and environmental causes of parkinsonism. *Occup. Med.*, **1992**, 7, 503–513.
7. Chinta, S.J.; Andersen, J.K.. Dopaminergic neurons. *Int. J. Biochem. Cell Biol.*, **2005**, 37, 942–946.
8. Dawson, T.M.; Dawson, V.L.. Molecular pathways of neurodegeneration in Parkinson's disease. *Science*, **2003**, 302, 819–822.
9. Nolano, M.; Provitera, V.; Estraneo, A.; Selim, M.M.; Caporaso, G.; Stancanelli, A.; Saltalamacchia, A.M.; Lanzillo, B.; Santoro, L.. Sensory deficit in Parkinson's disease: Evidence of a cutaneous denervation. *Brain*, **2008**, 131, 1903–1911.

10. Volpicelli-Daley, L.A.; Luk, K.C.; Patel, T.P.; Tanik, S.A.; Riddle, D.M.; Stieber, A.; Meaney, D.F.; Trojanowski, J.Q.; Lee, V.M.Y.. Exogenous a-synuclein fibrils induce Lewy body pathology leading to synaptic dysfunction and neuron death. *Neuron*, **2011**, 72, 57–71.
11. Berg, D.; Postuma, R.B.; Adler, C.H.; Bloem, B.R.; Chan, P.; Dubois, B.; Gasser, T.; Goetz, C.G.; Halliday, G.; Joseph, L.. MDS research criteria for prodromal Parkinson's disease. *Mov. Disord*., **2015**, 30, 1600–1611.
12. Cersosimo, M.G.; Benarroch, E.E.. Autonomic involvement in Parkinson's disease: pathology, pathophysiology, clinical features and possible peripheral biomarkers. *J. Neurol. Sci.*, **2012**, 313 (1-2), 57-63.
13. Shindo, K.; Kobayashi, F.; Miwa, M.; Nagasaka, T.; Takiyama, Y.; Shiozawa, Z.. Temporal prolongation of decreased skin blood flow causes cold limbs in Parkinson's disease, *J. Neural Transm.*, **2013**, 120 (3), 445-451.
14. Antonio-Rubio, I.; Madrid-Navarro, C.J.; Salazar-Lòpez, E.; Pèrez Navarro, M.J.; Sàez-Zea, C.; Gòmez-Milàn, E.; Mìnguez-Castellanos, A.; Escamilla-Sevilla, F.. Abnormal thermography in Parkinson's disease. *Parkinsonism Relat. D.*, **2015**, 21 (8), 852-857.
15. Møller Purup, M.; Knudsen, K.; Karlsson, P.; Skin Temperature in Parkinson's Disease Measured by Infrared Thermography. *Hindawi Parkinson's Disease*, **2020,** 2020, 1-7.
16. Anbalagan, B.; Karman Anantha, S.; Arjunan, S.P.; Balasubramanian, V.; Murugesan, M.; Kalpana, R.. A Non-Invasive IR Sensor Technique to Differentiate Parkinson's Disease from Other Neurological Disorders Using Autonomic Dysfunction as Diagnostic Criterion. *Sensors,* **2022**, 22 (1), 266.
17. Ring, E.F.J.; Ammer, K.. Infrared thermal imaging in medicine. *Physiol. Meas*., **2012**, 33 (3), 33-46.
18. Goldstein, D. S.; Sewell, L.; Sharabi, Y.. Autonomic dysfunction in PD: A window to early detection?. *J. Neurol. Sci.*, **2011**, 310, 118–122.
19. Cannuli, A.; Caccamo, M.T.; Magazù, S.. Modeling and Self-Organization Dynamics of Aggregation Processes in Acoustically Levitated Disaccharides Solutions. *AAPP Atti Accad. Pelorit. Pericol., Cl. Sci. Fis. Mat. Nat*., **2018**, 96 (S3, A3).